The intermediate-conductance calcium-activated potassium channel KCa3.1 contributes to atherogenesis in mice and humans

Kazuyoshi Toyama,[1] Heike Wulff,[2] K. George Chandy,[3] Philippe Azam,[2] Girija Raman,[2] Takashi Saito,[4] Yoshimasa Fujiwara,[5] David L. Mattson,[6] Satarupa Das,[6] James E. Melvin,[7] Phillip F. Pratt,[8] Ossama A. Hatoum,[9] David D. Gutterman,[1,10,11] David R. Harder,[1,6] and Hiroto Miura[1]

[1]Department of Medicine and Cardiovascular Center, Medical College of Wisconsin, Milwaukee, Wisconsin, USA. [2]Department of Pharmacology, University of California, Davis, Davis, California, USA. [3]Department of Physiology and Biophysics, University of California, Irvine, Irvine, California, USA. [4]Division of Cardiology, Akita Kumiai General Hospital, Akita, Japan. [5]Division of Cardiology, Fujiwara Memorial Hospital, Akita, Japan. [6]Department of Physiology, Medical College of Wisconsin, Milwaukee, Wisconsin, USA. [7]Center for Oral Biology, University of Rochester, Rochester, New York, USA. [8]Department of Anesthesiology, Medical College of Wisconsin, Milwaukee, Wisconsin, USA. [9]Department of Surgery B, Haemek Medical Center, Faculty of Medicine, Technion, Israel Institute of Technology, Haifa, Israel. [10]Departments of Pharmacology and Toxicology, Medical College of Wisconsin, Milwaukee, Wisconsin, USA. [11]Department of Veterans Affairs Medical Center, Milwaukee, Wisconsin, USA.

Atherosclerosis remains a major cause of death in the developed world despite the success of therapies that lower cholesterol and BP. The intermediate-conductance calcium-activated potassium channel KCa3.1 is expressed in multiple cell types implicated in atherogenesis, and pharmacological blockade of this channel inhibits VSMC and lymphocyte activation in rats and mice. We found that coronary vessels from patients with coronary artery disease expressed elevated levels of KCa3.1. In *Apoe*$^{-/-}$ mice, a genetic model of atherosclerosis, KCa3.1 expression was elevated in the VSMCs, macrophages, and T lymphocytes that infiltrated atherosclerotic lesions. Selective pharmacological blockade and gene silencing of KCa3.1 suppressed proliferation, migration, and oxidative stress of human VSMCs. Furthermore, VSMC proliferation and macrophage activation were reduced in *KCa3.1*$^{-/-}$ mice. In vivo therapy with 2 KCa3.1 blockers, TRAM-34 and clotrimazole, significantly reduced the development of atherosclerosis in aortas of *Apoe*$^{-/-}$ mice by suppressing VSMC proliferation and migration into plaques, decreasing infiltration of plaques by macrophages and T lymphocytes, and reducing oxidative stress. Therapeutic concentrations of TRAM-34 in mice caused no discernible toxicity after repeated dosing and did not compromise the immune response to influenza virus. These data suggest that KCa3.1 blockers represent a promising therapeutic strategy for atherosclerosis.

Introduction

Atherosclerosis is the ultimate pathological consequence of vascular remodeling and is associated with the activation of VSMCs and inflammatory cells (1–3). In atherosclerosis, VSMCs switch from a contractile state into cells that proliferate and migrate from the medial layer to form the fibrous cap overlying the atheromatous core of lipid in atherosclerotic plaques. Monocytes infiltrate the plaques, differentiate into macrophages, and contribute to atherogenesis by producing ROS, proteases, cytokines, and complement (1). Plasmacytoid dendritic cells in plaques activate infiltrating T lymphocytes, which in turn activate macrophages and kill ECs (2, 3). The development of new antiatherosclerotic therapies that modulate a target common to these pathophysiologically activated cells in atherogenesis — VSMCs, monocytes/macrophages, and T lymphocytes — would have substantial medical value.

The intermediate-conductance calcium-activated potassium channel composed of 4 KCa3.1 subunits and 4 calmodulin molecules is expressed in VSMCs (4–6), T lymphocytes (7), macrophages (8), and ECs (9), where it regulates membrane potential and calcium signaling (4, 10–12). We and others have reported that KCa3.1 mRNA expression is significantly increased in coronary arteries of rats with myocardial infarction (5) or hypertension (13) and of swine with early atherosclerosis (14).

Clotrimazole, an antifungal drug, blocks KCa3.1 with nanomolar potency but also potently inhibits cytochrome P450 enzymes (15). Two more-selective KCa3.1 blockers, which lack cytochrome P450 inhibitory activity, are the triarylmethanes TRAM-34 and ICA-17043 (15–18). KCa3.1 blockers inhibit VSMC proliferation and migration (6, 14), macrophage function (8, 19), T cell activation (15), and EC proliferation (9). In vivo blockade of KCa3.1 by clotrimazole or TRAM-34 prevents vascular restenosis following angioplasty by suppressing VSMC proliferation in rats (6), alleviates the symptoms of EAE by reducing T cell–mediated immune responses in mice (20), and inhibits angiogenesis by suppressing EC proliferation (9) that contributes to the progression of advanced atherosclerotic plaques (21). We therefore hypothesized that KCa3.1 might serve as a novel therapeutic target shared by these cell types implicated in atherogenesis.

Nonstandard abbreviations used: CAD, coronary artery disease; 1-EBIO, 1-ethyl-2-benzimidazolinone; HCA, human small coronary artery; KCa1.1, large-conductance calcium-activated potassium channel; KCa3.1, intermediate-conductance calcium-activated potassium channel; MCP-1, monocyte chemoattractant protein–1.

Conflict of interest: The authors have declared that no conflict of interest exists.

Citation for this article: *J. Clin. Invest.* **118**:3025–3037 (2008). doi:10.1172/JCI30836.

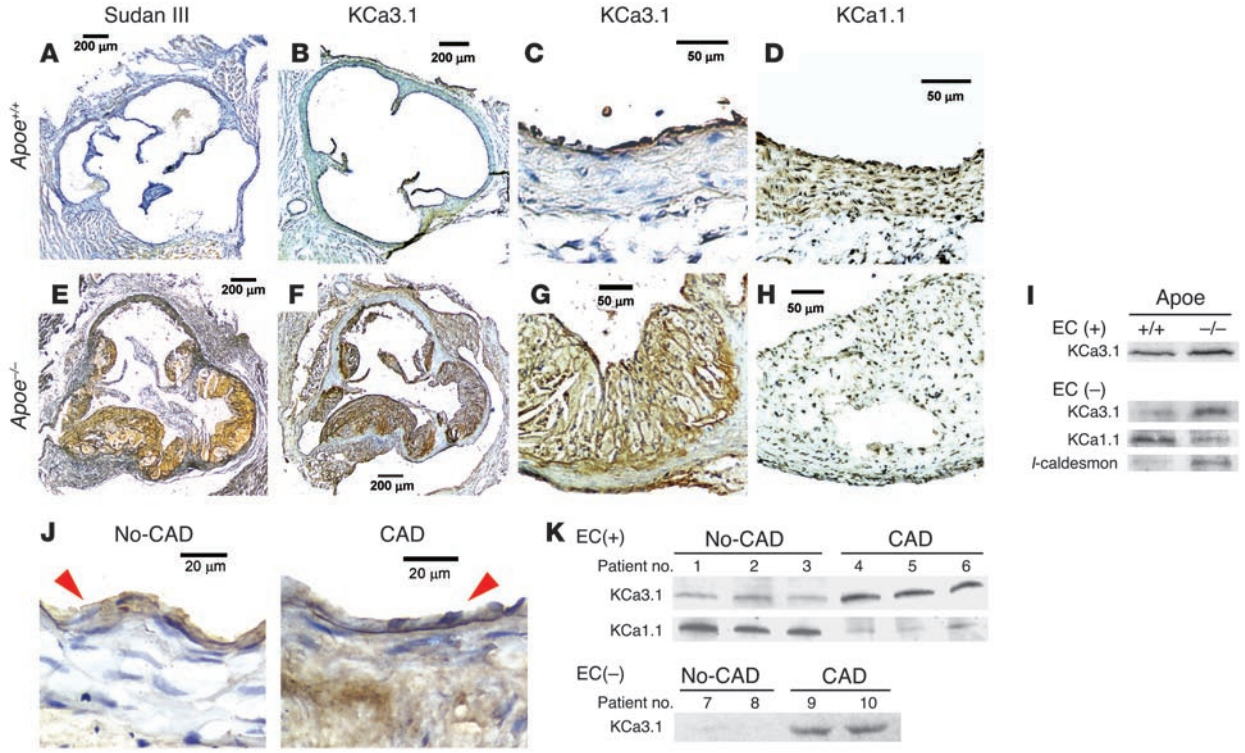

Figure 1

KCa3.1 upregulation in vessels of mice and humans with atherosclerosis. Representative images of *Apoe*$^{+/+}$ and *Apoe*$^{-/-}$ mouse aortic roots stained for lipid accumulation with Sudan III (**A** and **E**), KCa3.1 (**B** and **F**, **C** and **G**), and KCa1.1 (**D** and **H**). Sudan III staining is shown in yellow-orange and positive immunostaining in brown. Scale bars: 200 μm (**A**, **B**, **E**, and **F**), 50 μm (**C**, **D**, **G**, and **H**). (**I**) Western blot analysis of membrane fractions from *Apoe*$^{+/+}$ and *Apoe*$^{-/-}$ mouse aortic trees with or without ECs for KCa3.1 (MW, 46 kDa) and KCa1.1 (110 kDa) and of whole-cell lysates from those without ECs for *l*-caldesmon (~70 kDa). KCa3.1, 40 μg and KCa1.1, 30 μg membrane protein; *l*-caldesmon, 20 μg whole-cell lysates. Western blotting was repeated 3 times by pooling 3 aortas from each strain (9 aortas in each strain total) and showed similar results. (**J**) Representative images of KCa3.1 expression in HCAs from non-CAD (left) or CAD subject (right). Red arrowheads indicate EC layers that were positively stained for vWF (Supplemental Figure 3B). Scale bars: 20 μm. (**K**) Western blot analysis of KCa3.1 and KCa1.1 in EC-intact or -denuded HCAs with or without CAD (10 patients total). The 5 patients with no CAD are numbered 1–3, 7, and 8, and the 5 patients with CAD are numbered 4–6, 9, and 10. ECs were denuded in vessels of patients 7–10 (Supplemental Figure 3B).

Here, we measured KCa3.1 expression and activity in VSMCs and inflammatory cells in vessels of humans and mice with atherosclerosis. We examined whether pharmacological blockade, gene silencing, and KO of KCa3.1 inhibit cellular activation processes associated with atherogenesis. We explored whether in vivo KCa3.1 blockade with clotrimazole or TRAM-34 prevents the development of atherosclerosis without associated toxic side effects in *Apoe*$^{-/-}$ mice, which develop extensive atherosclerotic lesions in aortas that resemble human atherosclerosis (22). In this study, we demonstrate elevated expression levels of KCa3.1 in VSMCs, T cells, and macrophages in vessels of humans and mice with atherosclerosis. Pharmacological blockade and KO of KCa3.1 activity resulted in the suppression of proliferation, migration, and oxidative stress in VSMCs and macrophages. We shoed that KCa3.1 blockade inhibited the development of atherosclerosis in *Apoe*$^{-/-}$ mice.

Results

KCa3.1 expression is increased in atherosclerotic blood vessels. In aortas (aortic root) of *Apoe*$^{+/+}$ mice, no atherosclerotic plaques were observed on Sudan III staining for lipid accumulation (Figure 1A). Immunohistochemical analysis with a polyclonal Ab specific for KCa3.1 (Supplemental Figure 1; supplemental material available online with this article; doi:10.1172/JCI30836DS1) revealed that KCa3.1 expression was restricted to the intimal layer, and no KCa3.1 was detected in the medial layer (Figure 1, B and C). The intimal layer was defined by the expression of vWF, a marker of ECs, where the channel is normally expressed (9) (Supplemental Figure 2, middle). The medial layer was defined by the expression of α-SMA, a marker for VSMCs (Supplemental Figure 2, right), and by the expression of the large-conductance calcium-activated potassium channel KCa1.1 (Figure 1D). In *Apoe*$^{-/-}$ mouse aortas, large, yellow-orange atherosclerotic plaques were visible with Sudan III staining (Figure 1E). A serial section revealed robust KCa3.1 expression in the intimal and medial layers of the lesion area (Figure 1, F and G), while KCa1.1 expression in the vascular wall was faint (Figure 1H). Western blot analysis of EC-intact aortic trees (ascending aorta to abdominal aorta) showed increased expression of KCa3.1 in *Apoe*$^{-/-}$ mice compared with *Apoe*$^{+/+}$ mice (Figure 1I). EC denudation abolished KCa3.1 expression in *Apoe*$^{+/+}$ but not in *Apoe*$^{-/-}$ mouse aortas. EC-denuded aortas from *Apoe*$^{-/-}$ mice showed a significant elevation of KCa3.1 protein levels and reduced KCa1.1 levels compared with EC-denuded aortas from control *Apoe*$^{+/+}$ mice. EC denudation by this gentle method (23) did not cause the detachment of atherosclerotic plaques in the aor-

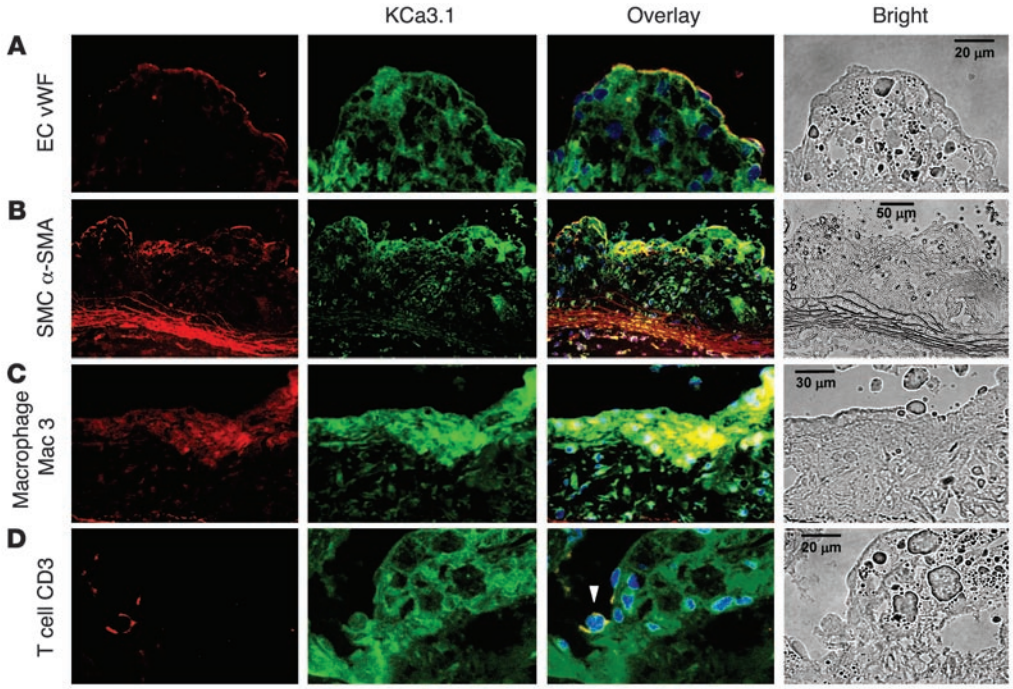

Figure 2
KCa3.1 localization in plaques of *Apoe*$^{-/-}$ mouse aortic roots. Double immunofluorohistochemical analysis of atherosclerotic plaques stained for vWF (**A**), α-SMA (**B**), Mac3 (**C**), and CD3 (**D**) with KCa3.1 staining. Representative images for each staining are in the far-left column (in red); KCa3.1 staining (in green) in the second column; overlays of the two (in yellow) in the third column; and bright-field images in the far-right column. Autofluorescence was not detectable in the plaques. Nuclei were stained blue with DAPI. White arrowhead indicates a T cell. Scale bars: 20 μm (**A** and **D**), 50 μm (**B**), 30 μm (**C**).

tic trees (Supplemental Figure 3). A comparison of EC-denuded aortas from control *Apoe*$^{+/+}$ mice and atherosclerotic *Apoe*$^{-/-}$ mice revealed a significant reduction in KCa1.1 and a parallel elevation of KCa3.1 and *l*-caldesmon, a marker of dedifferentiated, immature VSMCs (Figure 1I) (24). These data show a change in KCa subtype expression from KCa1.1 to KCa3.1 in VSMCs, paralleling their phenotypic conversion from a normal contractile state to a proliferative, dedifferentiated one in atherosclerosis.

A similar switch in KCa subtype expression was observed in human small coronary arteries (HCAs) from subjects with coronary artery disease (CAD), even though no plaques were present in these vessels. In subjects with no CAD, KCa3.1 was only present in the vWF^{+} intimal layer (Supplemental Figure 3), while it was expressed in both the intimal and medial layers in vessels from patients with CAD (Figure 1J). Western blot analysis was done on protein lysates from HCAs from 5 patients with CAD (patients 4–6, 9, and 10) and 5 patients with no CAD (patients 1–3, 7, and 8). EC-intact (patients 4–6) and -denuded (patients 9 and 10) HCAs from patients with CAD showed marked elevation of KCa3.1 protein levels and reduced levels of KCa1.1 compared with EC-intact (patients 1–3) and -denuded (patients 7 and 8) HCAs from patients without CAD (Figure 1K). KCa3.1 expression was abolished by EC denudation in non-CAD subjects but not in CAD subjects. These results in humans confirm the data in mice indicate that a change in vascular KCa subtype expression from KCa1.1 to KCa3.1 is a feature of atherosclerosis.

KCa3.1 is localized in vascular and inflammatory cells in plaques. Two-color immunofluorohistochemistry was performed in plaques of

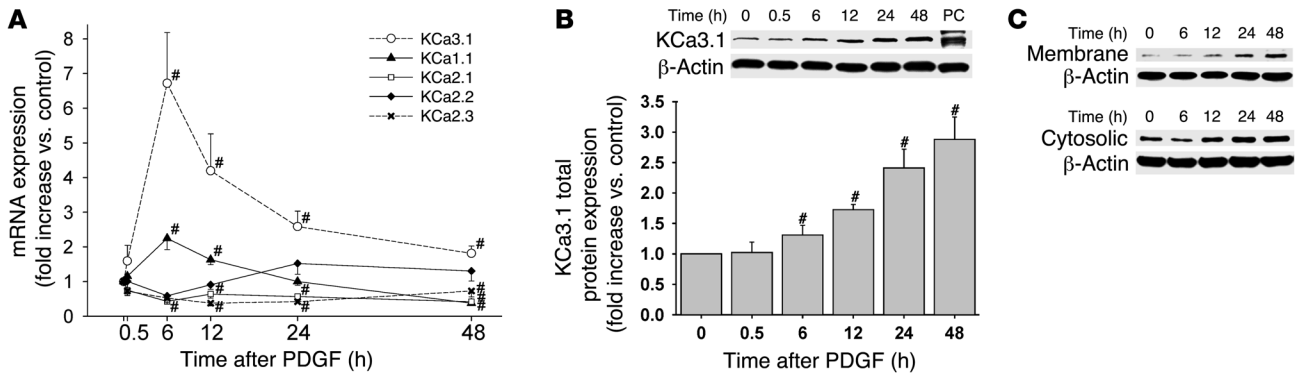

Figure 3
KCa3.1 upregulation in activated VSMCs. (**A**) Stimulation with 20 ng/ml PDGF increased KCa3.1 mRNA in human coronary SMCs. mRNA expression of KCa1.1, -2.1, -2.2, and -2.3 was unchanged or decreased. $n = 5–9$. (**B**) Total KCa3.1 protein expression (20 μg whole-cell lysates) was increased in VSMCs in a time-dependent fashion. $n = 9$. (**C**) KCa3.1 protein expression in membrane and cytosolic fractions (50 μg) was increased during PDGF stimulation. PC, positive controls. $^{\#}P < 0.05$ versus control.

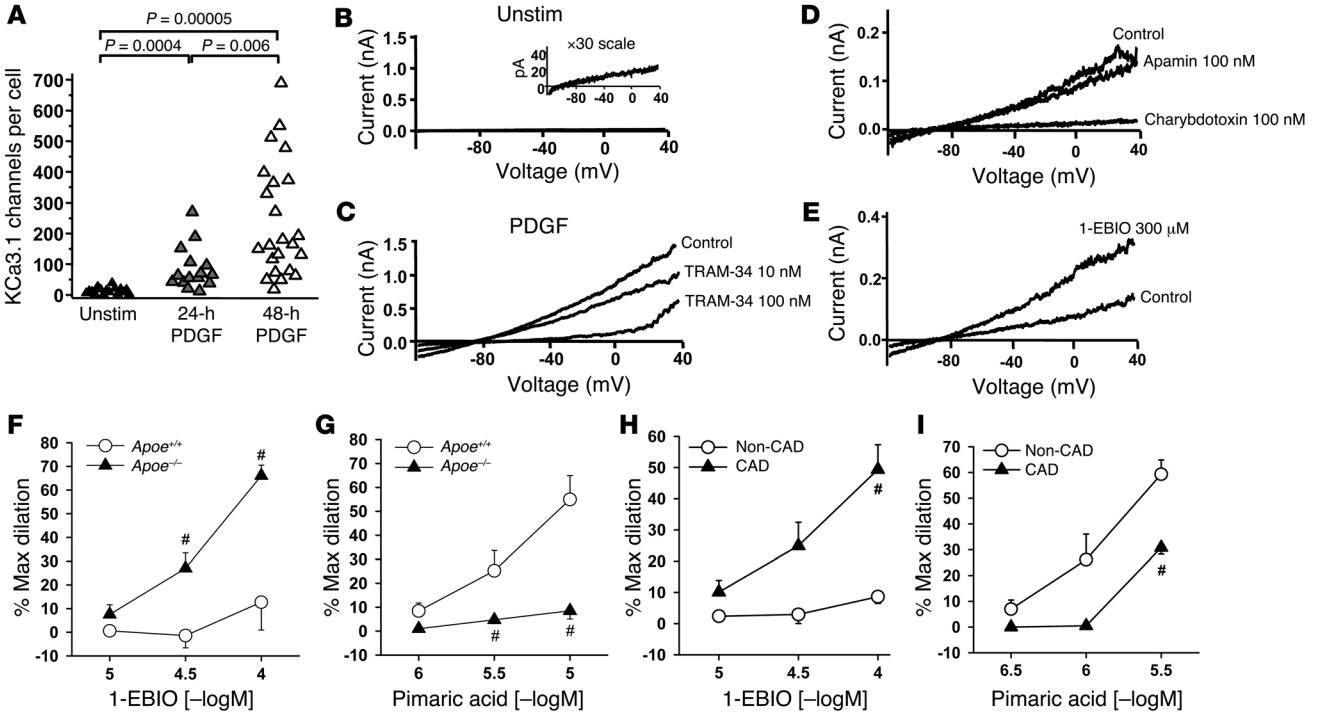

Figure 4

Increased KCa3.1 channel activity in activated VSMCs and in arteries from subjects with atherosclerosis. (**A**) Stimulation with PDGF increased KCa3.1 channel numbers in VSMCs. (**B**) Quiescent VSMCs demonstrated minimal KCa3.1 current. (**C**) The KCa3.1 current in PDGF-stimulated cells is blocked by TRAM-34 with an IC_{50} value (18 nM) similar to that obtained for the cloned channel. (**D**) The current was blocked by charybdotoxin (IC_{50}, 5 nM) but not by the small-conductance calcium-activated potassium channel (KCa2.1–2.3) blocker apamin. (**E**) The KCa3.1 activator 1-EBIO enhanced the amplitude of the current. (**F**–**I**) Vasodilations to KCa3.1 stimulation with 1-EBIO and KCa1.1 stimulation with pimaric acid in EC-denuded carotid artery segments of *Apoe*$^{-/-}$ mice (**F** and **G**) and in EC-denuded HCAs from CAD subjects (**H** and **I**). $^{\#}P < 0.05$ compared with *Apoe*$^{+/+}$ mice or non-CAD subjects. Max, maximum; [–logM], negative logarithm of the molar concentration; Unstim, unstimulated.

Apoe$^{-/-}$ mouse aortic sinus using cell-specific Abs to determine which cell types contribute to the increased KCa3.1 expression in atherosclerosis. KCa3.1 staining overlapped with vWF on the surface of intimal plaques (Figure 2A), indicating its expression in ECs. KCa3.1 staining also overlapped with α-SMA in the medial layer and in intimal plaques (Figure 2B), indicating its presence in VSMCs that had proliferated, migrated, and/or infiltrated into the intima. Macrophages, visualized in lesions by immunostaining for Mac3, also expressed KCa3.1 (Figure 2C), and T cells stained for CD3 in the lesions expressed KCa3.1 (Figure 2D, arrowhead). KCa3.1 localization in the medial layer was also observed in a variety of peripheral arteries from *Apoe*$^{-/-}$ mice, where plaques were not observed, as we had noted in HCAs. Taken together, these results demonstrate KCa3.1 expression in 3 of the major cell types (VSMCs, T cells, and macrophages) involved in the formation of atherosclerotic plaques.

Functional consequences of KCa3.1 expression in VSMCs. To study the role of KCa3.1 in the activation of VSMCs, we stimulated human coronary SMCs with PDGF, a mitogen widely used in vitro and in vivo (25). PDGF stimulation resulted in a time-dependent increase in KCa3.1 mRNA expression, peaking at 6 hours (Figure 3A). There was a corresponding increase in KCa3.1 protein expression in total cell lysates (Figure 3B) and in membrane and cytosolic fractions, peaking at 24–48 hours (Figure 3C). The delay between peak mRNA and protein expression likely reflects the time required for the functional channel to be synthesized, coassembled as tetramers with calmodulin, and trafficked to the membrane (7). A concomitant increase in *l*-caldesmon protein expression, a marker of dedifferentiated, immature VSMCs, was noted (data not shown). KCa1.1 mRNA increased slightly 6 and 12 hours after PDGF stimulation and then decreased significantly at 48 hours (Figure 3A). The mRNA expression of small-conductance calcium-activated potassium channels (KCa2.1–2.3) remained unchanged or decreased following stimulation with PDGF (Figure 3A). Protein expression was not detectable for KCa2.1–2.3 in any of 4 experiments and for KCa1.1 in 7 of 8 experiments before or after stimulation with PDGF (20 μg whole cell lysates; data not shown).

Whole-cell patch-clamp experiments corroborated the mRNA and protein expression data. PDGF induced a substantial increase in functional KCa3.1 channels in VSMCs (Figure 4A). KCa3.1 currents were elicited in VSMCs using a ramp protocol from –120 mV to 40 mV and 3 μM free calcium in the pipette (Figure 4, B–E). While KCa3.1 currents were barely detectable in unstimulated cells (Figure 4B), the amplitude of the KCa3.1 current increased 24 and 48 hours after PDGF stimulation (Figure 4C). The current was blocked by TRAM-34 (IC_{50}, 18 nM) (Figure 4C), a specific blocker of KCa3.1 channels (15) (Supplemental Figure 4), and by charybdotoxin (Figure 4D) with an IC_{50} value (5 nM) similar to that obtained for the cloned KCa3.1 channel (15). Apamin, a blocker of KCa2.1–2.3, had no effect on the current (Figure 4D). Iberiotoxin, a specific blocker of KCa1.1, blocked a minor fraction of the current (data not shown), confirming the small amount of KCa1.1

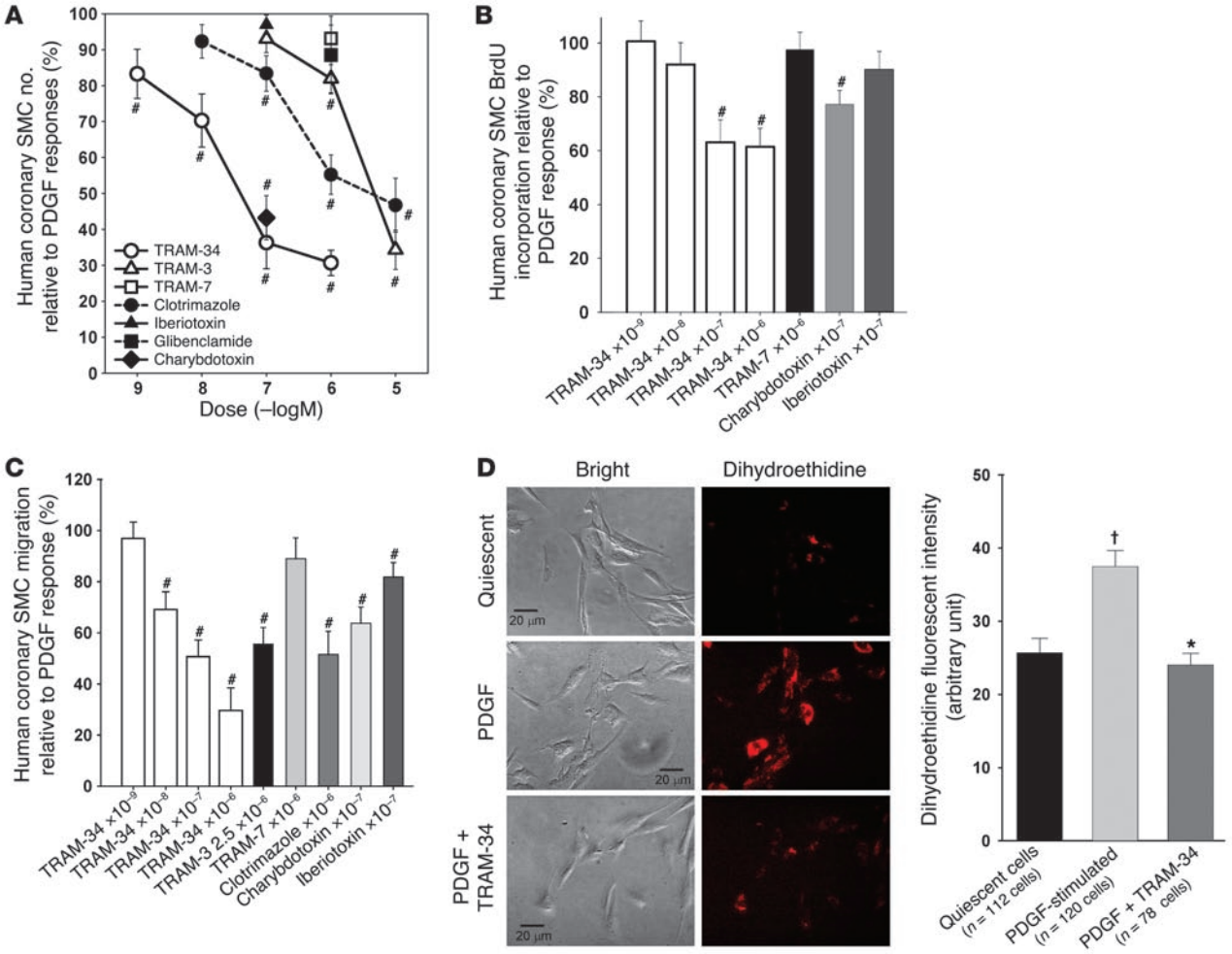

Figure 5

KCa3.1 blockade prevents VSMC activation. KCa3.1 blockers suppressed PDGF-stimulated proliferation (**A**, cell count assay; n = 6–9), DNA synthesis (**B**, BrdU incorporation; n = 6–17), migration (**C**; n = 6–7), and ROS production (**D**) of human coronary SMCs. TRAM-7 (an inactive analog of TRAM-34), iberiotoxin (KCa1.1 blocker), and glibenclamide (ATP-sensitive potassium channel [K_{ATP}] blocker) had no effect. (**A**–**C**). $^{\#}P < 0.05$ versus PDGF alone; $^{\dagger}P < 0.0005$ versus quiescent cells; $^{*}P < 0.0005$ versus PDGF-stimulated cells. Scale bars: 20 μm.

protein in these cells. 1-Ethyl-2-benzimidazolinone (1-EBIO), an activator of KCa3.1 channels (26), increased the amplitude of the current (Figure 4E). VSMCs in the quiescent state expressed an average of 15 KCa3.1 channels/cell, which increased after PDGF stimulation to 85 channels/cell at 24 hours and 256 channels/cell at 48 hours (Figure 4A).

Due to the increased KCa3.1 expression in the medial layer of atherosclerotic vessels, 1-EBIO elicited robust vasodilatory responses in EC-denuded carotid artery segments from atherosclerotic *Apoe*$^{-/-}$ compared with *Apoe*$^{+/+}$ mice (Figure 4F; maximum dilation, 66% ± 4% versus 13% ± 12% at 100 μM; $P < 0.05$; n = 5–6). Similar results were obtained with EC-denuded HCAs from CAD patients versus non-CAD subjects (Figure 4H; 49% ± 8% versus 9% ± 2% at 100 μM; $P < 0.05$; n = 10–11). Conversely, because KCa1.1 is decreased in the medial layer of mouse and human atherosclerotic vessels, the KCa1.1 opener pimaric acid (27) evoked markedly reduced vasodilation in vessels from *Apoe*$^{-/-}$ compared with *Apoe*$^{+/+}$ mice (Figure 4G; 9% ± 3% versus 55% ± 10% at 10 μM; $P < 0.05$; n = 5–7) and CAD patients compared with subjects without CAD (Figure 4I; 31% ± 3% versus 59% ± 6% at 3 μM; $P < 0.05$; n = 4–5). Taken together, the calcium dependence of the current, its characteristic pharmacology, the mRNA and protein data, and the vasomotor responses to 1-EBIO verify the presence of functional KCa3.1 channels in activated VSMCs. These results suggest that the enhanced levels of KCa3.1 in atherosclerotic vessels may in part be a consequence of the upregulation of this channel during VSMC activation.

We used pharmacological blockade, gene silencing with siRNAs, and gene disruption to define the functional consequences of KCa3.1 upregulation in VSMCs. In the pharmacological experiments, TRAM-34, at concentrations that block the KCa3.1 channel, suppressed PDGF-induced proliferation (cell count assay; Figure 5A), de novo DNA synthesis (BrdU incorporation assay; Figure 5B), and migration (Figure 5C) of VSMCs in a dose-dependent fashion. Other KCa3.1 blockers (TRAM-3, clotrimazole, and charybdotoxin) had similar effects. TRAM-7 (an inactive analog of TRAM-34) (15), iberiotoxin, and glibenclamide (a blocker of ATP-sensitive potassium [K_{ATP}] channels) had no discernible effect on

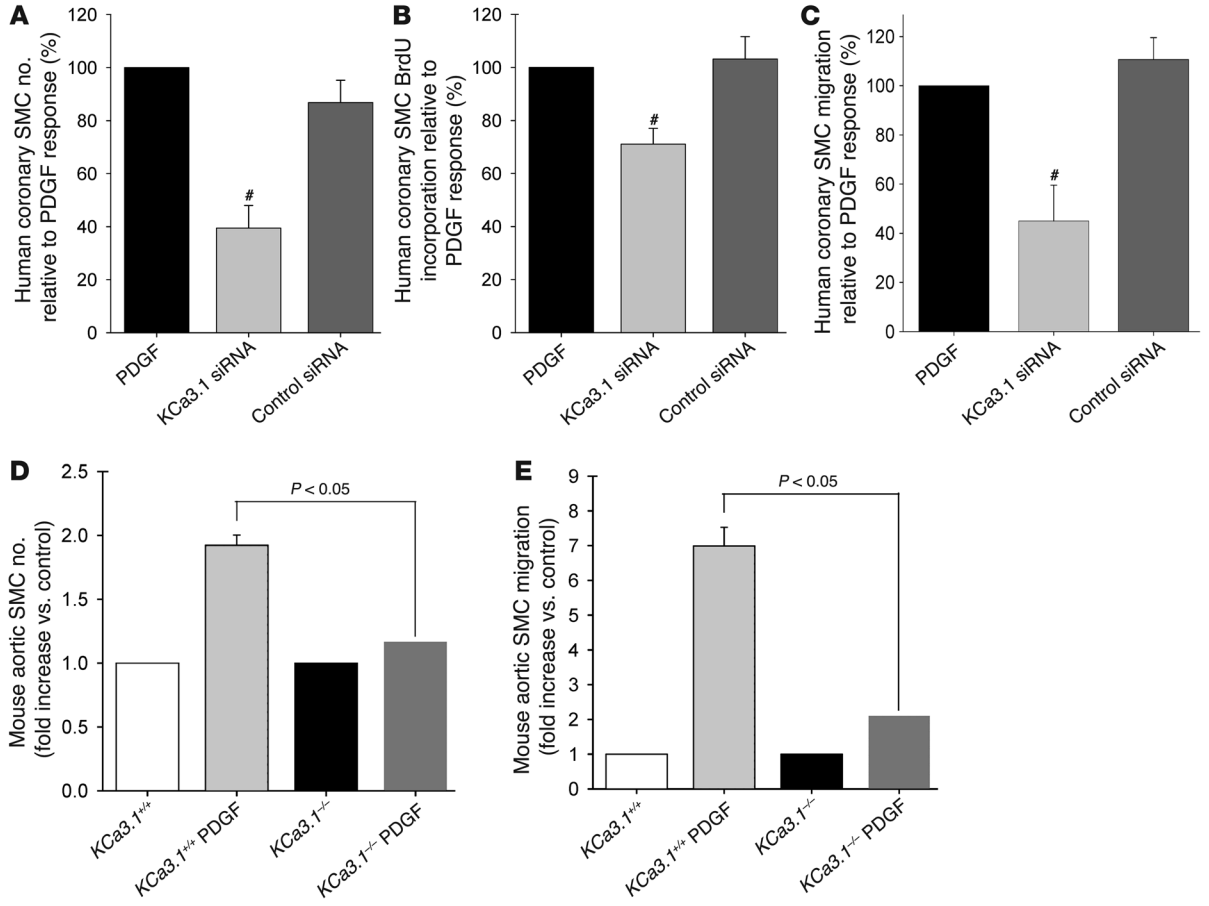

Figure 6

KCa3.1 gene silencing or KO prevents VSMC activation. KCa3.1 gene silencing by specific siRNA transfection reduced PDGF-stimulated proliferation (**A**, cell count assay; $n = 6$), DNA synthesis (**B**, BrdU incorporation; $n = 8$), and migration (**C**; $n = 6$) of human coronary SMCs. $^{\#}P < 0.05$ versus PDGF. Aortic VSMCs from *KCa3.1*$^{-/-}$ mice exhibited reduced proliferative (**D**; $n = 7$–8) and migratory (**E**; $n = 7$–8) responses to PDGF compared with VSMCs from *KCa3.1*$^{+/+}$ mice.

these processes. FBS also consistently induced strong cell cycle progression of VSMCs following 24-hour stimulation, with cell numbers decreasing in G_0/G_1 phase (FBS: 63% ± 1% of cells, $P < 0.05$ versus quiescent: 89% ± 1%; $n = 4$) and increasing in S phase. TRAM-34 suppressed FBS-induced cell cycle progression at the transition from G_0/G_1 to S phase (FBS plus TRAM-34: 72% ± 0%, $P < 0.05$ versus FBS). Since VSMC activation is associated with increased superoxide production (28), we also measured superoxide levels in VSMCs (Figure 5D) following 48-hour stimulation with PDGF. TRAM-34 reduced PDGF-stimulated superoxide production to a level comparable to that in quiescent cells. None of the KCa3.1 blockers (TRAM-34, TRAM-3, clotrimazole, charybdotoxin) altered the viability of VSMCs as judged by trypan blue exclusion (Supplemental Figure 5), and in a previous report, TRAM-34 was shown not to exhibit cytotoxicity against a panel of 9 cell lines and primary T cells (15). Similar results were obtained with gene silencing. KCa3.1-specific siRNA inhibited PDGF-stimulated increases in KCa3.1 mRNA and protein levels (Supplemental Figure 6) and suppressed the proliferation (Figure 6A), de novo DNA synthesis (Figure 6B), and migration (Figure 6C) of VSMCs, whereas control siRNA had no effect. Gene disruption studies also support a role for KCa3.1 in regulating VSMC proliferation and migratory responses. VSMCs from *KCa3.1*$^{-/-}$ mouse aortas exhibited reduced proliferative and migratory responses to PDGF compared with VSMCs from *KCa3.1*$^{+/+}$ mice (Figure 6, D and E).

Functional consequences of KCa3.1 expression in macrophages. Our in vitro studies showed that mouse macrophages but not monocytes express KCa3.1. Expression of KCa3.1 was detectable by immunofluorescence in thioglycollate-elicited peritoneal macrophages of *Apoe*$^{-/-}$ mice but not in monocytes isolated from PBMCs of these mice (Figure 7A). In Transwell experiments, TRAM-34 and clotrimazole suppressed monocyte chemoattractant protein–1–induced (MCP-1–induced) migration of macrophages from *Apoe*$^{-/-}$ mice in a dose-dependent manner (Figure 7B). Moreover, the migratory response of peritoneal macrophages from *KCa3.1*$^{-/-}$ mice was significantly smaller than in *KCa3.1*$^{+/+}$ mice (Figure 7C). These data together with the results of VSMCs presented in Figures 5 and 6 and our previously published work on the role of KCa3.1 in T cells (7, 15) highlight the important role of KCa3.1 channels in the activation of VSMCs, macrophages, and T cells. A therapeutic strategy based on the selective targeting of KCa3.1 channels in these 3 cell types may therefore be beneficial in treatment of atherosclerosis.

In vivo KCa3.1 blockade therapy prevents atherosclerosis. We tested the antiatherosclerotic potential of KCa3.1 blockade in *Apoe*$^{-/-}$ mice.

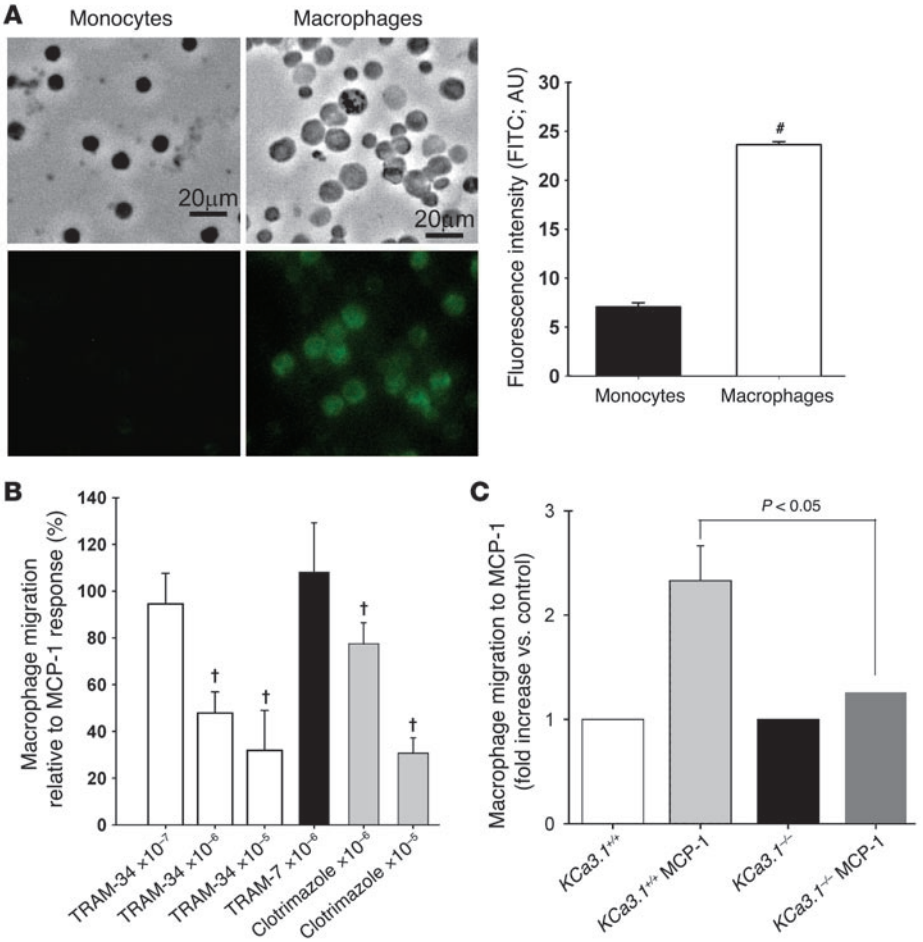

Figure 7
KCa3.1 blockade or gene KO prevents macrophage activation. (**A**) KCa3.1 is abundantly expressed in macrophages but little in monocytes. Autofluorescence was not detectable in macrophages. $^{\#}P < 0.05$ versus monocytes; $n = 3$ mice, 445 monocytes, 1,572 macrophages. (**B**) TRAM-34 and clotrimazole dose-dependently inhibited macrophage migration to MCP-1. $^{\dagger}P < 0.05$ versus MCP-1 alone; $n = 4–11$. (**C**) Macrophage migration to MCP-1 was significantly reduced in *KCa3.1*$^{-/-}$ mice compared with *KCa3.1*$^{+/+}$ mice. $n = 8–9$. Scale bars: 20 μm.

Clotrimazole or TRAM-34 dissolved in peanut oil was administered once daily (120 mg/kg, s.c.) (6) for 12 weeks. We used 120 mg/kg of each blocker because the bioavailability following s.c. administration was poor (0.5% of the availability after i.v. administration) and because the circulating half-life of these compounds in mice was short (1 hour) (Supplemental Figure 7). We chose this s.c. route because it was more convenient and less stressful on the mice than i.p. administration for a 12-week study. After a single s.c. injection of 120 mg/kg, total plasma levels of TRAM-34 averaged 782, 720, 112, and 88 nM at 1, 2, 12, 24 hours (Supplemental Figure 7C), which would be sufficient to inhibit VSMCs, macrophages, and T cells. Due to their high lipophilicity, both clotrimazole and TRAM-34 accumulated in the body after repeated administration, and after 12 weeks of treatment, total plasma levels 24 hours after the last drug administration were 1,719 ± 354 nM for clotrimazole ($n = 8$) and 866 ± 48 nM for TRAM-34 ($n = 6$). Considering TRAM-34's protein binding of 98% (data not shown), the free plasma concentration of TRAM-34 was around the IC_{50} for channel blockade for most of our study.

Long-term KCa3.1 blockade therapy with clotrimazole or TRAM-34 strikingly reduced atherosclerosis in *Apoe*$^{-/-}$ mouse aortas and carotid arteries. Representative images of atherosclerotic lesions stained in yellow-orange with Sudan III in aortic trees (left panels) and carotid arteries (right panels) are shown in Figure 8A, with quantitative measurements of atherosclerotic lesions summarized in Figure 8B ($n = 10–14$ mice). No lesions were observed in control *Apoe*$^{+/+}$ mice. Aortas of *Apoe*$^{-/-}$ mice treated for 12 weeks with vehicle developed extensive atherosclerotic lesions in carotid arteries and in the aortic trees. Mice treated with clotrimazole or TRAM-34 for 12 weeks showed a statistically significant reduction in the atherosclerotic lesion area, both in the various segments of the aorta and in the carotid arteries (Figure 8B).

Plaques in aortic roots where more advanced lesions developed in *Apoe*$^{-/-}$ mice (29) were examined histologically to determine the effect of KCa3.1 blockade therapy in *Apoe*$^{-/-}$ mice treated with TRAM-34 versus vehicle ($n = 9–10$). In a vehicle-treated mouse, large plaques stained with Sudan III were visible in the cross section (Figure 9A). Atherosclerotic lesions contained α-SMA^{+} VSMCs, Mac3^{+} macrophages, CD3^{+} T cells, and acellular/necrotic areas (30) (Figure 2 and Figure 9, B–E, respectively). Representative images of an aortic root from a TRAM-34–treated mouse are shown in Figure 9, F–J. The plaques were much smaller than in vehicle-treated *Apoe*$^{-/-}$ mice (Figure 9F), showing smaller areas stained for α-SMA, Mac3, and CD3 and smaller acellular/necrotic areas (Figure 9, G–J, respectively). Statistical analysis of the histological data showed that TRAM-34 significantly decreased total lesion area, α-SMA^{+} area, Mac3^{+} area, the number of infiltrating CD3^{+} T cells, and the size of the acellular/necrotic area (Table 1). Since excess superoxide production in the medial VSMCs plays a causal role in diminishing NO bioactivity and impairing EC-dependent vasodilation (31), we measured superoxide production in the vessels of vehicle- and TRAM-34–treated *Apoe*$^{-/-}$ mice. The therapy significantly reduced

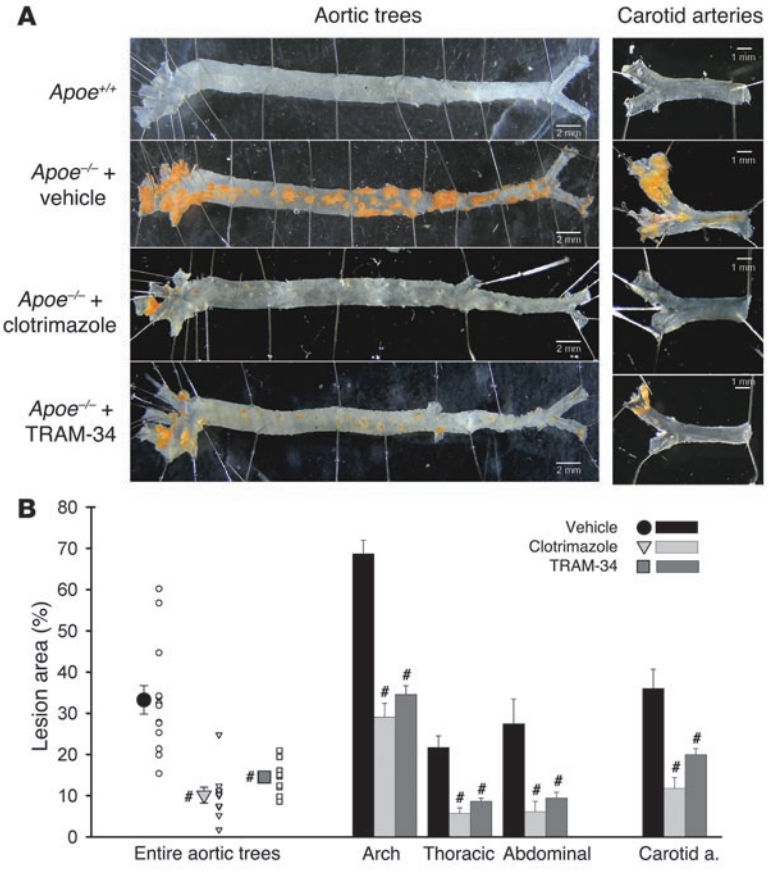

Figure 8
KCa3.1 blockade therapy prevents the development of atherosclerosis in *Apoe*$^{-/-}$ mice. (**A**) Representative images of atherosclerotic lesions in aortic trees from the ascending aorta to the iliac bifurcation (left) and in carotid arteries from the common carotid artery to the cervical bifurcation (right; stained yellow-orange with Sudan III) of *Apoe*$^{+/+}$ and *Apoe*$^{-/-}$ mice treated with vehicle, clotrimazole, or TRAM-34. (**B**) Quantitative measurements of atherosclerotic lesion area (atherosclerotic lesion area/whole vascular area). *Apoe*$^{-/-}$ mice treated with vehicle: 33% ± 3%, n = 14, versus clotrimazole-treated *Apoe*$^{-/-}$ mice: 10% ± 2%, n = 10, $^{\#}P < 0.05$; and TRAM-34–treated *Apoe*$^{-/-}$ mice: 15% ± 1%, n = 12, $^{\#}P < 0.05$. Scale bars: 2 mm (aortic trees), 1 mm (carotid arteries).

superoxide production compared with vehicle treatment (Figure 9K), consistent with its inhibition of superoxide production in activated VSMCs (Figure 5D). Because ECs contribute only 10% of total superoxide generated in whole vascular walls in aortas of *Apoe*$^{-/-}$ mice (32), the inhibitory effect is most likely due to suppression of superoxide production by VSMCs and macrophages (8, 28, 31). Thus, TRAM-34 and clotrimazole may decrease atherosclerosis and the necrotic area by inhibiting VSMCs, macrophages, and T cells.

Safety profile of KCa3.1 blockers. To determine the safety profile of clotrimazole and TRAM-34, we monitored clinical parameters (body weight, heart weight, BP, and heart rate), blood chemistry, blood counts, and histopathology in *Apoe*$^{+/+}$ mice and in *Apoe*$^{-/-}$ mice treated with vehicle or with clotrimazole or TRAM-34 during the 12-week trial (Supplemental Tables 1 and 2). Clotrimazole and TRAM-34 ameliorated atherosclerosis in *Apoe*$^{-/-}$ mice, even though the cholesterol levels remained elevated. In *Apoe*$^{-/-}$ mice, TRAM-34 did not cause any discernible change in the clinical parameters, blood counts, or blood chemistry compared with vehicle, whereas a body weight reduction of 17% was seen in clotrimazole-treated mice, which was accompanied by a significant increase in the levels of total protein, globulin, calcium, and the anion gap. In parallel toxicological experiments, normal C57BL/6J (*Apoe*$^{+/+}$) mice treated with TRAM-34 for 4 weeks did not exhibit any signs of toxicity or show visible abnormalities in the aortas, macroscopic organ damage, or any histopathological changes in the organs analyzed (Supplemental Table 3). Because of its immunosuppressive effects on T cells and macrophages, KCa3.1 blockers might compromise the immune response to acute infections. However, in rats infected intranasally with influenza virus, the viral clearance was delayed by dexamethasone but not by TRAM-34 (Supplemental Figure 9), indicating that KCa3.1 blockade with TRAM-34 does not affect the immune response to infectious agents. Additional information on the safety profile of KCa3.1 blockers is provided in Supplemental Results.

Discussion

We have used a multifaceted strategy to identify a novel therapeutic approach for atherosclerosis, a disease responsible for nearly 50% of deaths in the Western world (1). Our approach is based on targeting KCa3.1 calcium-activated potassium channels in 3 activated cell types — VSMCs, macrophages, and T cells — that are implicated in the pathogenesis of atherosclerosis. We demonstrate augmented KCa3.1 expression in vessels from patients with CAD and atherosclerotic vessels from *Apoe*$^{-/-}$ mice. We used pharmacological blockers of the channel, siRNA gene silencing, and gene KO of KCa3.1 to show that the channel plays an essential role in the activation processes of VSMCs and macrophages. We have previously reported a critical role for KCa3.1 channels in the activation of CCR7^{+} naive and central memory T cells (7, 15). Most importantly, we showed that long-term therapy with TRAM-34 or clotrimazole results in a striking reduction in the size of atherosclerotic lesions in the aorta and the carotid arteries of *Apoe*$^{-/-}$ mice without altering the blood lipid profile. Histological analysis revealed a significant reduction in the level of VSMCs, macrophages, T cells, and necrosis in the lesions. The selective KCa3.1 blocker TRAM-34 did not cause any toxic side effects in *Apoe*$^{-/-}$ or *Apoe*$^{+/+}$ mice, consistent with the excellent safety profile in humans of another KCa3.1-specific blocker, ICA-17043, which is/was in clinical trials for the treatment of sickle cell disease (17, 18) and asthma.

VSMC proliferation and migration play an important role in the development of atherosclerotic lesions in humans and in *Apoe*$^{-/-}$ mice (1, 29). We and others have previously reported in rats and swine that KCa3.1 expression increases in VSMCs during vascular remodeling following balloon catheter injury (6), myocardial infarction (5), hypertension (13), and early atherosclerosis (14). Here we report a significant increase in KCa3.1 expression in atherosclerotic vessels in humans and mice. In the aortas of *Apoe*$^{+/+}$ mice and in coronary vessels of patients without CAD, KCa3.1 channels are normally localized in ECs, while the medial layer

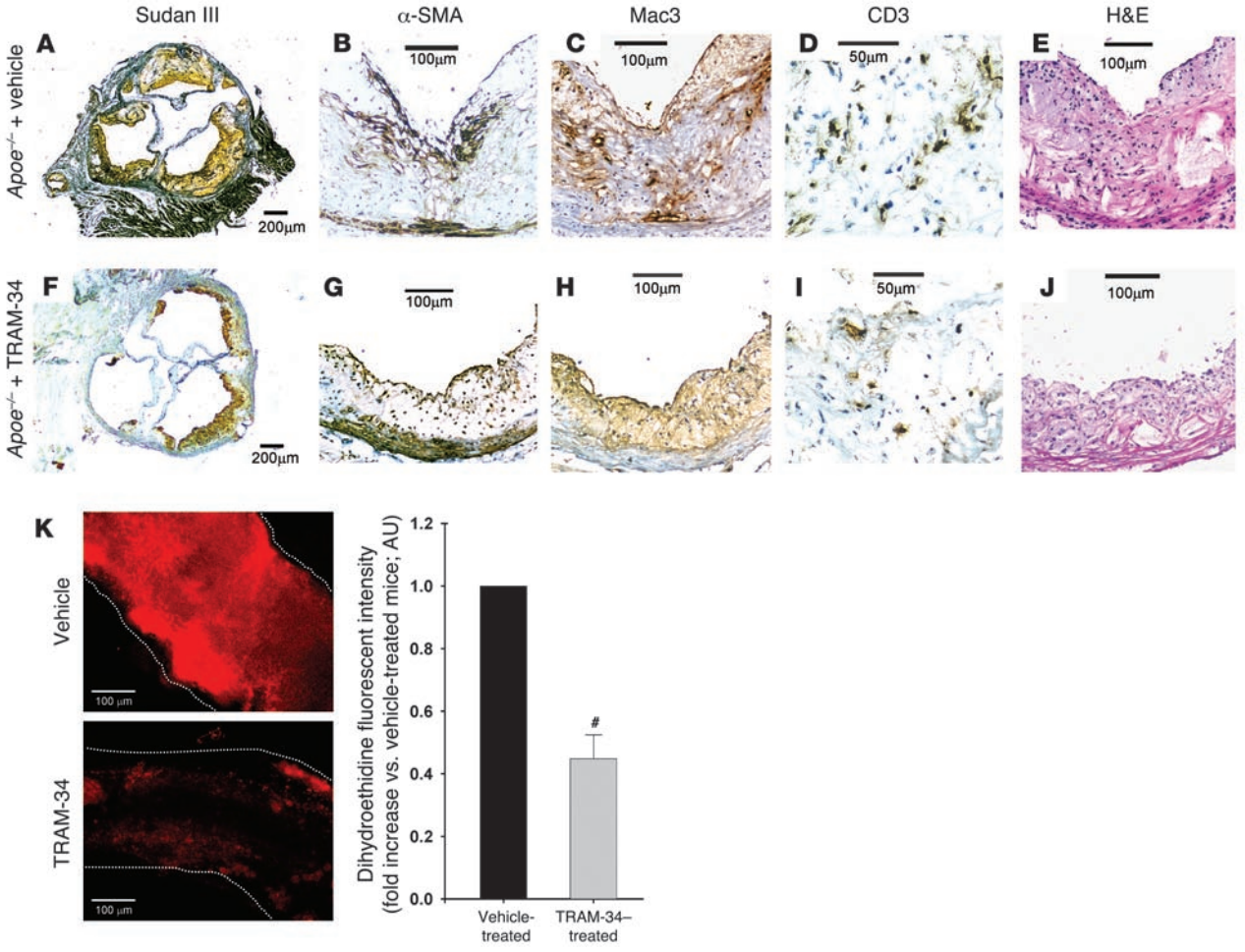

Figure 9

Antiatherosclerotic effect of KCa3.1 blockade therapy with TRAM-34 in *Apoe*$^{-/-}$ mice. Typical atherosclerotic lesions in the aortic root of a mouse treated with vehicle (**A**–**E**) or TRAM-34 (**F**–**J**). Serial 5-μm sections were stained with Sudan III (**A** and **F**); Abs specific to VSMCs (α-SMA; **B** and **G**), macrophages (Mac3; **C** and **H**), or T cells (CD3; **D** and **I**); or H&E (**E** and **J**). (**K**) Left: Representative images comparing fluorescence intensity of dihydroethidine, representing the production of superoxide in isolated iliac arteries of *Apoe*$^{-/-}$ mice treated with vehicle or TRAM-34. Vessels with no intimal plaques were isolated, incubated with dihydroethidine, and laid on glass slides, and images were taken perpendicularly to vessels. Each vessel is traced with white dotted lines. Right: Summary of fluorescence intensities (normalized to vehicle-treated *Apoe*$^{-/-}$ mice) in 7 arteries of each group. Dihydroethidine fluorescence intensity was significantly decreased in TRAM-34–treated *Apoe*$^{-/-}$ mouse arteries. $^{\#}P < 0.05$ versus vehicle. Scale bars: 200 μm (**A** and **F**), 100 μm (**B**, **C**, **E**, **G**, **H**, **J**, and **K**), 50 μm (**D** and **I**).

contains contractile VSMCs that express KCa1.1 channels (4). In contrast, vessels from *Apoe*$^{-/-}$ mice and patients with CAD showed decreased expression of KCa1.1 together with increased expression of KCa3.1 in the medial layer. We also detected KCa3.1 expression in VSMCs that had proliferated and migrated into intimal plaques of *Apoe*$^{-/-}$ mouse aortas. Since PDGF-induced VSMC activation is accompanied by an increase in KCa3.1 expression, the enhanced level of KCa3.1 in atherosclerotic plaques may in part be a consequence of the upregulation of this channel during the activation process. Increased expression of KCa3.1 is involved in driving proliferation and migration of VSMCs, as these channels open in response to small fluctuations in intracellular $[Ca^{2+}]$ ($[Ca^{2+}]_i$) (4) and their opening enhances the electrochemical driving force for capacitative Ca^{2+} entry (11), thereby sustaining the high $[Ca^{2+}]_i$ levels and membrane hyperpolarization required for VSMC activation through gene transcription and DNA synthesis (33).

PDGF induced a dramatic increase in KCa3.1 mRNA, protein, and functional channel expression in VSMCs. Other growth factors that are released in atherosclerotic lesions, such as EGF, IGF-1, and bFGF, have a similar effect on KCa3.1 expression (6, 34). The suppression by KCa3.1 blockers of PDGF- and FBS-induced proliferation, de novo DNA synthesis, migration, ROS production, and G_0/G_1-S cell cycle transition of VSMCs suggests a rationale for blocking these channels in VSMCs as a method to treat atherosclerosis.

The necrotic core of atherosclerotic lesions is made up primarily of dead macrophages and is rich in inflammatory cytokines, and the number of macrophages in lesions is an important measure of atherosclerotic burden. Macrophages contribute to plaque formation and to plaque progression by producing cytokines, ROS, proteases, complement, and inflammatory factors such as MCP-1 and leukotriene B4 that are critical for recruitment of additional macrophages and their persistence within plaques (1, 35). We

Table 1
Characteristics of atherosclerotic lesions in aortic roots from *Apoe*$^{-/-}$ mice

	Treatment	
	Vehicle (n = 9)	TRAM-34 (n = 10)
Total lesion area (×10^3 μm^2)	477 ± 30	257 ± 31^A
SMC-positive area (×10^3 μm^2)	119 ± 16	43 ± 6^A
Macrophage-positive area (×10^3 μm^2)	219 ± 20	94 ± 11^A
T cell no. (per 10^3 μm^2)	2.3 ± 0.3	1.2 ± 0.2^A
Necrotic area (×10^3 μm^2)	70 ± 21	36 ± 10^A

Data are mean ± SEM. $^A P < 0.05$ versus vehicle.

found many Mac3$^+$ macrophages in intimal plaques of atherosclerotic vessels in *Apoe*$^{-/-}$ mice that also expressed KCa3.1. In a Transwell assay, MCP-1–induced migration of macrophages was inhibited by KCa3.1 blockade with TRAM-34 or clotrimazole and by KO of KCa3.1, and in vivo therapy with these blockers in *Apoe*$^{-/-}$ mice reduced macrophage infiltration into atherosclerotic lesions by approximately 60%. Our results confirm earlier in vitro studies that defined KCa3.1's role in the migration of macrophages and in their production of ROS and cytokines (8, 10). Both TRAM-34 and clotrimazole inhibited MCP-1–induced macrophage migration less potently than they inhibited PDGF-induced VSMC proliferation and migration. This difference may be due to the cell types involved. The proliferation of VSMCs is inhibited by TRAM-34 at the range between 10 and 100 nM as shown by us (Figure 5, A and B) and others (6). In contrast, between 500 and 1,000 nM TRAM-34 is required to suppress the proliferation in T lymphocytes (7), possibly because of the contributions of other channels to the maintenance of the membrane potential. Using the same reasoning, macrophages might be less sensitive to TRAM-34 because of channel redundancy. Taken together, these findings highlight the important functional role for KCa3.1 in macrophages and provide an additional rationale for targeting KCa3.1 in macrophages as a therapy for atherosclerosis.

Macrophages and plasmacytoid dendritic cells initiate adaptive immune responses in intimal plaques by presenting antigens to T cells and by secreting the potent immunoregulatory cytokine IFN-α (2, 3). As a result, T cells activate and secrete proatherogenic cytokines such as IFN-γ and IL-2 (36–38). Under the influence of IFN-α, T cells express TNF-related apoptosis-inducing ligand (TRAIL) on their surfaces, which enables them to kill VSMCs (2). The importance of T cells to atherosclerosis development is controversial. A recent study has demonstrated accelerated and severe atherosclerosis in *Apoe*$^{-/-}$ mice crossed with TGF-β receptor$^{-/-}$ mice; atherosclerotic lesions in these mice contain increased numbers of T cells and activated macrophages, and the level of circulating T cell cytokines is enhanced (39). IFN-γ, a cytokine secreted by T lymphocytes, induces expression of MCP-1 and apoptosis of macrophages (40). We found many CD3$^+$ T cells in intimal plaques of atherosclerotic vessels in *Apoe*$^{-/-}$ mice. Histological analysis showed that the CD3$^+$ T cells in atherosclerotic lesions stained positively for KCa3.1. These KCa3.1$^+$ T cells are likely to be activated CCR7$^+$ naive and central memory T cells that express high numbers (~500/cell) of KCa3.1 channels (41); the 10–20 KCa3.1 channels per T cell found in resting T cells are unlikely to be detected by immunohistochemistry. In vivo therapy with TRAM-34 in *Apoe*$^{-/-}$ mice reduced CD3$^+$ T cell infiltration into atherosclerotic lesions including necrotic areas by approximately 50%. The mechanism underlying this effect of TRAM-34 is possibly both a direct effect on T cells and an indirect effect on macrophages that recruit T cells to the lesion. We previously reported that TRAM-34 suppresses IFN-γ and IL-2 production and proliferation of CCR7$^+$ naive and central memory T cells (7). The suppression of cytokine production might reduce the inflammatory processes within atherosclerotic lesions. The recent discovery that KCa3.1 traffics to the immune synapse during antigen presentation suggests that the channel plays an important role in early signaling events in T cells (42). Although the role of KCa3.1 channels in T cell migration has not been determined yet, this channel plays a role in the migration of other cells, including mast cells and macrophages (19, 43, 44).

Our in vitro experiments and immunohistochemical findings in *Apoe*$^{-/-}$ mice and in coronary vessels in patients with CAD strongly argue that TRAM-34's antiatherosclerotic effect is mediated in part by a combined suppression of VSMC activation and the inflammatory processes involved in atherogenesis. Based on the clinical parameters we monitored in the mice, we can exclude changes in lipid homeostasis or hemodynamics as contributors to TRAM-34's therapeutic activity. Since KCa3.1 is involved in EC proliferation and angiogenesis (9) that contribute to the progression of advanced atherosclerotic plaques (21), the inhibition of angiogenesis in larger plaques may also contribute to TRAM-34's therapeutic effect. Given the role of KCa3.1 in mast cell migration (43), we also cannot exclude an effect of TRAM-34 on mast cells that can contribute to atherogenesis.

A key issue for any long-term therapy is the balance between efficacy and safety. Although blockade of KCa3.1 would appear to provide a good approach for atherosclerosis therapy, KCa3.1 is also present in many other cell types, raising the possibility that KCa3.1 blockers could have adverse side effects. We assessed this in several ways. First, TRAM-34 was tested by specificity screen on 30 receptors and transporters and was found to be a highly specific KCa3.1 blocker (Supplemental Figure 4). Previous patch-clamp studies had shown that TRAM-34 exhibits selectivity for KCa3.1 channels that is more than 1,000-fold greater than that for other potassium, sodium, and calcium channels (15). Second, clotrimazole and TRAM-34 did not reduce viability of human T cells, VSMCs, macrophages, and ECs, and we previously reported its lack of cytotoxicity on a panel of 9 cell lines (15). Third, repeated administration of clotrimazole or TRAM-34 at a pharmacological dose (120 mg/kg) to *Apoe*$^{+/+}$ or *Apoe*$^{-/-}$ mice for approximately 4–12 weeks did not produce any discernible change in blood counts, blood chemistry, or histopathology of any organ tested, consistent with other studies in mice and rats (6, 9, 15). In particular, KCa3.1 blockade therapy with clotrimazole or TRAM-34 did not change BP or cause left-ventricular hypertrophy in *Apoe*$^{+/+}$ and *Apoe*$^{-/-}$ C57BL/J mice or Lewis rats, unlike KCa3.1 KO in mice, which produces a 7-mmHg increase in BP and mild cardiac hypertrophy (45). Our results are consistent with reports that ICA-17043 and clotrimazole do not cause cardiovascular changes in humans, rats, and mice (17, 18, 46–48). In *KCa3.1*$^{-/-}$ mice, the gene was deleted, which may have caused compensatory changes during development, and the functional effect of such a deletion will be substantially different from that of pharmacological blockade, which varies during the day, depending on the pharmacokinetic properties of the blocker. Fourth, we showed that TRAM-34 treat-

ment did not compromise the immune response to influenza viral infection, which causes significant morbidity and mortality globally. The normal clearance of influenza virus in TRAM-34–treated rats likely results from the redundancy in the multiple cell types and mechanisms involved in viral clearance. Furthermore, repeat dosing of TRAM-34 for 28 days or KCa3.1 deficiency in mice did not deplete immune cells in the spleen or thymus (49) (Supplemental Figure 8). The lack of toxicity in humans administered an escalating dose of the TRAM-34 analog ICA-17043 (17, 18) supports our results.

Statins and drugs currently on clinical trails such as ezetimibe and PPARγ agonists are expected to exert their effects on very early processes of atherogenesis (cholesterol absorption, cell surface receptors, and signaling pathways). In contrast, KCa3.1 is upregulated specifically in many of the cell types (VSMCs, T cells, macrophages, and mast cells) implicated in atherogenesis and is a major modulator of calcium influx that is necessary for substantially maintaining cellular activation processes such as proliferation, migration, and cytokine production following activation of receptors and the Rho/Ras-dependent and -independent signal transduction pathways (50, 51). We have previously reported that cardiovascular remodeling induced by hypertension is associated with KCa3.1 upregulation consisting of an early peak (days) and a late increase (weeks). Treatment with statin inhibits the early increase but not the late increase in KCa3.1 expression (13). Thus, KCa3.1 blockers are likely to induce antiatherosclerotic effects in both early and late phases through mechanisms different from those of statins. Treatment with KCa3.1 blockers alone or in combination with statins might represent new therapeutic approaches for the management of atherosclerosis.

In summary, the expression and activity of KCa3.1 are increased in VSMCs, macrophages, and T cells in coronary arteries from subjects and in aortas of *Apoe*$^{-/-}$ mice with atherosclerosis. The increased KCa3.1 activity plays a crucial role in regulating the proliferation, migration, and ROS and cytokine production of these cell types that contribute to atherogenesis. KCa3.1 blockers markedly reduce the development of atherosclerosis in *Apoe*$^{-/-}$ mice without associated toxicity. Our data provide a compelling rationale for developing KCa3.1 blockers as a novel therapy for atherosclerosis.

Methods

Materials. The information on reagents and Abs other than KCa3.1 Ab is provided in Supplemental Methods.

KCa3.1 Ab. The polyclonal primary Ab against human and mouse KCa3.1 was obtained from sera of rabbits immunized using oligopeptides with the following amino acid sequence: H-LNASYRSIGALNQVRC-NH2 (S4–S5 of human and mouse KCa3.1). The specificity of this Ab for KCa3.1 was verified by Western blotting and immunofluorescence (Supplemental Figure 1). To generate immunoabsorbed serum, purified anti-KCa3.1 Ab was incubated with its corresponding peptide for 60 or 120 minutes at 37°C or room temperature. We titrated each preparation of affinity-purified Ab to the range of 0.05–5.0 μg/ml before performing immunofluorescence or Western blotting experiments.

Animals. Male mice (*Apoe*$^{+/+}$ [n = 16] and *Apoe*$^{-/-}$ [n = 78] C57BL/6J mice; The Jackson Laboratory) were used as a model of in vivo atherosclerosis. *Apoe*$^{-/-}$ mice were weaned at 4 weeks of age onto a high-cholesterol diet (1.25% cholesterol, 0% cholate, and 21% fat; 42% kcal as fat; Harlan Teklad) and treated with daily s.c. injection of clotrimazole (120 mg/kg/d), TRAM-34 (120 mg/kg/d), or vehicle (peanut oil) for 12 weeks (6, 9). Littermate *Apoe*$^{+/+}$ mice were used as controls. In separate experiments, male mice (*KCa3.1*$^{+/+}$, n = 11 and *KCa3.1*$^{-/-}$, n = 12) (49) were used for in vitro experiments involving VSMCs and macrophages. Mice were provided food and water ad libitum and maintained on a 12-hour light/120-hour dark cycle. All animal experiments were approved by the Institutional Animal Care and Use Committee of the Medical College of Wisconsin.

Mouse vessel acquisition. Mice anesthetized with sodium pentobarbital were sacrificed by cardiac puncture. Isolation of aortas was performed as previously described (52). Under a microscope, common carotid arteries, first and second branches of external carotid arteries (150~250 μm in internal diameter, 3–5 mm in length) and iliac arteries were removed and placed immediately into cold (4°C) HEPES buffer (53).

Human vessel acquisition. HCAs (150~1,000 μm internal diameter, 1–2 mm length; n = 26) were isolated as reported previously (53–55). The schedules and procedures of cardiac surgery (coronary artery bypass graft, valve replacement, and congenital repair) were obtained from the hospitals mentioned below. Right atrial appendages, removed as discarded tissues for cannulation during cardiopulmonary bypass, were obtained at the time of cardiac surgery and immediately placed in cold (4°C), well-oxygenated HEPES buffer consisting of (in mM/l) 138.0 NaCl, 4.0 KCl, 1.6 $CaCl_2$, 1.2 KH_2PO_4, 1.2 $MgSO_4$, 0.026 Na_2EDTA, 10.0 HEPES, and 6 glucose, pH 7.4, before being brought to the laboratory. Using forceps and scissors, HCAs were dissected from adjacent tissue and cleaned of cardiomyocytes, fat, and connective tissues in cold HEPES buffer under a dissecting microscope. All protocols were approved by the local institutional review boards at the Medical College of Wisconsin, the Department of Veterans Affairs Medical Center, St. Luke's Hospital, St. Joseph's Hospital, Sinai Samaritan Hospital, and St. Mary's Hospital in Milwaukee, Wisconsin, and at Waukesha Memorial Hospital in Waukesha, Wisconsin, USA.

Quantification of atherosclerosis. For en face analysis of atherosclerosis (30, 32, 39), excised aortic trees (from ascending aorta to iliac bifurcation) and right carotid arteries (common carotid artery to cervical bifurcation) were dissected free from surrounding tissues, opened longitudinally, and pinned onto a silicon-coated dish filled with HEPES buffer. They were fixed with 4% paraformaldehyde in PBS overnight and stained 3 hours in 1.0% (vol/wt) Sudan III solution. Images were collected using a digital camera (C-755; Olympus).

Histological analysis of aortic sinus and HCAs were examined in cross sections (30, 32, 39). Aortic roots including aortic valve and sinus or HCAs were isolated and frozen in OCT compound. Every other section (thickness, 6 μm) was mounted and fixed with 4% paraformaldehyde in PBS. The lipid accumulated in the plaques was stained with Sudan III. H&E-stained sections were used to determine the total acellular/necrotic area in the lesions (30). Immunostains were visualized using avidin-biotin HRP visualization systems (VECTASTAIN Elite ABC kits or M.O.M. immunodetection kit; Vector Laboratories) and Mayer's hematoxylin solution (Sigma-Aldrich) for counterstaining or using FITC- or Texas red–conjugated secondary Abs (53). Controls for nonspecific immunostaining were performed in the absence of primary Abs. Each section was photographed using a Nikon E600 microscope with a Spot R/T cooled CCD digital camera (Diagnostic Instruments Inc.) or a Nikon E200 inverted fluorescence microscope. No immunostaining was detected in negative controls (no primary Abs), except for autofluorescence from extracellular elastin/collagen fibers in the sections.

For quantitative analysis of histological characteristics in the plaques, the stained area as a percentage of total area in each aortic tree and carotid artery and the immunostained area (μm^2), the number of immunostained cells (nuclei), and acellular/necrotic area (μm^2) in each section of aortic roots were determined using MetaMorph imaging software (Molecular Devices); and the mean lesion area or the cell number per section per mouse were calculated for each group of mice.

Videomicroscopy. Vasodilator responses of HCAs and mouse carotid arteries were examined by videomicroscopy as previously described (53–55). Vessels pressurized at 60 mmHg for HCAs and at 40 mmHg for mouse arteries were preconstricted with acetylcholine (HCAs) or U46619 (mouse arteries), and vasodilations to 1-EBIO and pimaric acid were studied.

EC denudation. Mouse aortas were dissected free of adventitial fat and connective tissue and cut open longitudinally. ECs were removed without detachment of plaques by gently rubbing the intimal surface with a moist cotton swab under a microscope, which was followed by rinsing, as previously reported (23). ECs in HCAs and mouse arteries were also mechanically denuded using a modification of a method used previously by us (53–55). Removal of ECs was confirmed by lack of immunostaining for vWF and by abolishment of EC-dependent vasodilation and is described in Supplemental Methods and Supplemental Figure 3.

VSMC culture. Human coronary artery SMCs were purchased and cultured according to the manufacturer's instructions (Cambrex Inc.). Patient information is not released by the company. All experiments were performed between passages 5 and 7. Mouse aortic SMCs were isolated as previously reported (56) and described in Supplemental Methods. After the quiescent state of cells was achieved by 48-hour incubation in serum-free medium (SmBM), cells were stimulated with 20 ng/ml PDGF in each assay.

Monocyte and macrophage isolation. PBMCs were isolated from peripheral blood of *Apoe*$^{-/-}$ mice by modified density-gradient centrifugation using Nycoprep (Nycomed) (57) and by positive selection using CD11b magnetic cell separation system beads (Miltenyi Biotec) (58). Macrophages from the peritoneal cavity of thioglycollate-injected *Apoe*$^{-/-}$, *KCa3.1*$^{+/+}$, and *KCa3.1*$^{-/-}$ mice were isolated 4 days after the injection (59).

Real-time PCR. Total RNA from VSMCs was isolated with TRIzol Reagent (Invitrogen), and real-time PCR analysis (iCycler; Bio-Rad) was performed for quantification of transcripts for human KCa1.1, -2.1, -2.2, -2.3, and -3.1 (GenBank accession number NM002250) and for GAPDH (AF106860) as previously described (6). Primer sequences and the reaction conditions are available in Supplemental Methods.

Immunocytochemistry. VSMCs, monocytes, and macrophages seeded onto a Lab-Tek Chamber Slide system (Nunc) were immunolabeled for KCa3.1. VSMCs adherent to the chamber and monocytes and macrophages spun and deposited onto the chamber by Cytospin were immediately fixed with 4% paraformaldehyde and dried. The remainder of the immunostaining methodology was performed as described previously (53). No immunostaining or autofluorescence was seen in negative controls (no primary Abs).

siRNA transfection. siRNA transfection was performed as previously reported (60) and described in Supplemental Methods.

Western blotting. Total cell lysates or membrane and cytosolic fractions (20–50 μg) of VSMCs, HCAs, or mouse aortic trees were analyzed by Western blotting. The gels were stained in Coomassie blue to confirm equal protein loading. Rat brain extract, PC-12 cell lysate, and COLO 320DM cell lysate (Santa Cruz Biotechnology Inc.) were used as positive controls.

Cell proliferation and migration. Cell proliferation (cell count and BrdU incorporation assays) and migration assays were performed as previously reported (59). VSMCs were stimulated with 20 ng/ml PDGF for 8 hours in the migration assay and for 48 hours in the proliferation assay. Macrophages were stimulated with 1 nM MCP-1 for 90 minutes in the migration assay. All control experiments (PDGF or MCP-1 alone) were performed in the presence of vehicle for blockers.

Fluorescence detection of ROS. Fluorescence microscopy was performed as previously described (55). Changes in superoxide generation in vessels and VSMCs were assessed by measuring dihydroethidine fluorescence intensity.

Electrophysiology. VSMCs were patch clamped in the whole-cell mode of the patch-clamp technique. KCa3.1 currents were elicited by dialysis with 3×10^{-6} M of free calcium as previously described (6, 15).

Cell cycle analysis by flow cytometry. Flow cytometry was performed using VSMCs stimulated with 10% FBS as previously reported (33). Cells stained with 50 μg/ml propidium iodide were analyzed with a BD FACScan. Data were analyzed with CELLQuest software.

Statistics. All data are expressed as mean ± SEM. Data other than those from the vasodilation studies were statistically analyzed by paired *t* test; ANOVA for 1-way, 2-way, and repeated measures; and nonparametric tests for data that were not distributed normally, where appropriate. Vasodilation data were analyzed as previously reported (53, 55). Agonist-induced dilations are expressed as a percentage, with 100% dilation representing the change from the constricted diameter to the maximal diameter obtained by addition of papaverine (10^{-4} mol/l). Statistical comparisons of maximum percent vasodilation were performed using paired *t* test, whenever applicable. A 2-factor repeated-measures ANOVA was used to compare dose-response (factor 1) relationships between the treatment groups (factor 2). Interactions, if any, were noted between dose and treatments groups. Corollary dose-specific comparisons were tested using a Bonferroni-adjusted *t* test whenever the interactions were statistically significant. All procedures were done using "proc mixed" or "proc glm" programs of SAS for Windows version 8.2. Statistical significance was defined as a value of $P < 0.05$.

Acknowledgments

This study was supported by American Heart Association (AHA) Northland Affiliate Beginning Grant-in-Aid 0360035Z, an Advancing a Healthier Wisconsin grant from the Medical College of Wisconsin, and NIH grant R01 HL080173-01A2 to H. Miura; NIH grants P01 HL68769-02 and P50 HL65203 and a Veterans Administration Merit Review grant to D.D. Gutterman; NIH grant R01 GM076063 and a Translational Technology Grant from the University of California Davis to H. Wulff; NIH grants R01 NS48252 and AHA 0455025Y to K.G. Chandy; NIH grants R01 DE09692 and R37 DE08921 to J.E. Melvin; and NIH grants P01 HL68769-02 and P01 HL59996 to D.R. Harder. The authors wish to thank Daniel Homerick for excellent technical assistance in performing the HPLC/MS analysis; Stephen Griffey for expert pathology; and the Division of Cardiothoracic Surgery at the Medical College of Wisconsin, the Cardiovascular Surgery Associates of Milwaukee, the Cardiothoracic Surgery Group of Milwaukee, the Midwest Heart Surgery Institute, and the Wisconsin Heart Group for providing surgical specimens.

Received for publication November 3, 2006, and accepted in revised form June 25, 2008.

Address correspondence to: Hiroto Miura, Department of Medicine and Cardiovascular Center, Medical College of Wisconsin, 8701 Watertown Plank Road, Milwaukee, Wisconsin 53226, USA. Phone: (414) 456-5639; Fax: (414) 456-6572; E-mail: hmiura@mcw.edu.

1. Libby, P. 2002. Inflammation in atherosclerosis. *Nature.* **420**:868–874.
2. Niessner, A., et al. 2006. Pathogen-sensing plasmacytoid dendritic cells stimulate cytotoxic T-cell function in the atherosclerotic plaque through interferon-alpha. *Circulation.* **114**:2482–2489.
3. Benagiano, M., et al. 2003. T helper type 1 lymphocytes drive inflammation in human atherosclerotic lesions. *Proc. Natl. Acad. Sci. U. S. A.* **100**:6658–6663.
4. Neylon, C.B., Lang, R.J., Fu, Y., Bobik, A., and Reinhart, P.H. 1999. Molecular cloning and characterization of the intermediate-conductance Ca^{2+}-activated K^+ channel in vascular smooth muscle: relationship between KCa channel diversity and smooth muscle cell function. *Circ. Res.* **85**:e33–e43.
5. Saito, T., et al. 2002. Role of augmented expression of intermediate-conductance Ca^{2+}-activated K^+ channels in postischaemic heart. *Clin. Exp. Pharma-*

col. Physiol. **29**:324–329.
6. Kohler, R., et al. 2003. Blockade of the intermediate-conductance calcium-activated potassium channel as a new therapeutic strategy for restenosis. *Circulation.* **108**:1119–1125.
7. Ghanshani, S., et al. 2000. Up-regulation of the IKCa1 potassium channel during T-cell activation. Molecular mechanism and functional consequences. *J. Biol. Chem.* **275**:37137–37149.
8. Schmid-Antomarchi, H., et al. 1997. Extracellular ATP and UTP control the generation of reactive oxygen intermediates in human macrophages through the opening of a charybdotoxin-sensitive Ca2+-dependent K+ channel. *J. Immunol.* **159**:6209–6215.
9. Grgic, I., et al. 2005. Selective blockade of the intermediate-conductance Ca^{2+}-activated K^+ channel suppresses proliferation of microvascular and macrovascular endothelial cells and angiogenesis in vivo. *Arterioscler. Thromb. Vasc. Biol.* **25**:704–709.
10. Hanley, P.J., et al. 2004. Extracellular ATP induces oscillations of intracellular Ca^{2+} and membrane potential and promotes transcription of IL-6 in macrophages. *Proc. Natl. Acad. Sci. U. S. A.* **101**:9479–9484.
11. Fanger, C.M., et al. 2001. Calcium-activated potassium channels sustain calcium signaling in T lymphocytes. Selective blockers and manipulated channel expression levels. *J Biol. Chem.* **276**:12249–12256.
12. Sharma, N.R., and Davis, M.J. 1994. Mechanism of substance P-induced hyperpolarization of porcine coronary artery endothelial cells. *Am. J. Physiol.* **266**:H156–H164.
13. Terata, Y., et al. 2003. Pitavastatin inhibits upregulation of intermediate conductance calcium-activated potassium channels and coronary arteriolar remodeling induced by long-term blockade of nitric oxide synthesis. *Pharmacology.* **68**:169–176.
14. Tharp, D.L., Wamhoff, B.R., Turk, J.R., and Bowles, D.K. 2006. Upregulation of intermediate-conductance Ca^{2+}-activated K^+ channel (IKCa1) mediates phenotypic modulation of coronary smooth muscle. *Am. J. Physiol. Heart Circ Physiol.* **291**:H2493–H2503.
15. Wulff, H., et al. 2000. Design of a potent and selective inhibitor of the intermediate-conductance Ca^{2+}-activated K^+ channel, IKCa1: a potential immunosuppressant. *Proc. Natl. Acad. Sci. U. S. A.* **97**:8151–8156.
16. Stocker, J.W., et al. 2003. ICA-17043, a novel Gardos channel blocker, prevents sickled red blood cell dehydration in vitro and in vivo in SAD mice. *Blood.* **101**:2412–2418.
17. Ataga, K.I., et al. 2008. Efficacy and safety of the Gardos channel blocker, Senicapoc (ICA-17043), in patients with sickle cell anemia. *Blood.* **111**:3991–3997.
18. Ataga, K.I., et al. 2006. Dose-escalation study of ICA-17043 in patients with sickle cell disease. *Pharmacotherapy.* **26**:1557–1564.
19. Schilling, T., Stock, C., Schwab, A., and Eder, C. 2004. Functional importance of Ca^{2+}-activated K^+ channels for lysophosphatidic acid-induced microglial migration. *Eur. J. Neurosci.* **19**:1469–1474.
20. Reich, E.P., et al. 2005. Blocking ion channel KCNN4 alleviates the symptoms of experimental autoimmune encephalomyelitis in mice. *Eur. J. Immunol.* **35**:1027–1036.
21. Bochkov, V.N., et al. 2006. Oxidized phospholipids stimulate angiogenesis via autocrine mechanisms, implicating a novel role for lipid oxidation in the evolution of atherosclerotic lesions. *Circ. Res.* **99**:900–908.
22. Plump, A.S., et al. 1992. Severe hypercholesterolemia and atherosclerosis in apolipoprotein E-deficient mice created by homologous recombination in ES cells. *Cell.* **71**:343–353.
23. Kolodgie, F.D., Virmani, R., Rice, H.E., and Mergner, W.J. 1990. Vascular reactivity during the progression of atherosclerotic plaque. A study in Watanabe heritable hyperlipidemic rabbits. *Circ. Res.* **66**:1112–1126.
24. Owens, G.K. 1995. Regulation of differentiation of vascular smooth muscle cells. *Physiol. Rev.* **75**:487–517.
25. Bornfeldt, K.E., et al. 1994. Insulin-like growth factor-I and platelet-derived growth factor-BB induce directed migration of human arterial smooth muscle cells via signaling pathways that are distinct from those of proliferation. *J. Clin. Invest.* **93**:1266–1274.
26. Syme, C.A., Gerlach, A.C., Singh, A.K., and Devor, D.C. 2000. Pharmacological activation of cloned intermediate- and small- conductance Ca^{2+}-activated K^+ channels. *Am. J. Physiol. Cell Physiol.* **278**:C570–C581.
27. Imaizumi, Y., et al. 2002. Molecular basis of pimarane compounds as novel activators of large-conductance Ca^{2+}-activated K^+ channel alpha-subunit. *Mol. Pharmacol.* **62**:836–846.
28. Pandolfi, A., et al. 2003. Phenotype modulation in cultures of vascular smooth muscle cells from diabetic rats: association with increased nitric oxide synthase expression and superoxide anion generation. *J. Cell. Physiol.* **196**:378–385.
29. Nakashima, Y., Plump, A.S., Raines, E.W., Breslow, J.L., and Ross, R. 1994. ApoE-deficient mice develop lesions of all phases of atherosclerosis throughout the arterial tree. *Arterioscler. Thromb.* **14**:133–140.
30. Zhao, B., et al. 2007. Macrophage-specific transgenic expression of cholesteryl ester hydrolase significantly reduces atherosclerosis and lesion necrosis in Ldlr–/– mice. *J. Clin. Invest.* **117**:2983–2992.
31. Miller, F.J., Jr., Gutterman, D.D., Rios, C.D., Heistad, D.D., and Davidson, B.L. 1998. Superoxide production in vascular smooth muscle contributes to oxidative stress and impaired relaxation in atherosclerosis. *Circ. Res.* **82**:1298–1305.
32. Ozaki, M., et al. 2002. Overexpression of endothelial nitric oxide synthase accelerates atherosclerotic lesion formation in apoE-deficient mice. *J. Clin. Invest.* **110**:331–340.
33. Simons, M., Ariyoshi, H., Salzman, E.W., and Rosenberg, R.D. 1995. c-myb affects intracellular calcium handling in vascular smooth muscle cells. *Am. J. Physiol.* **268**:C856–C868.
34. Cheong, A., et al. 2005. Downregulated REST transcription factor is a switch enabling critical potassium channel expression and cell proliferation. *Mol. Cell.* **20**:45–52.
35. Subbarao, K., et al. 2004. Role of leukotriene B4 receptors in the development of atherosclerosis: potential mechanisms. *Arterioscler. Thromb. Vasc. Biol.* **24**:369–375.
36. Gupta, S., et al. 1997. IFN-gamma potentiates atherosclerosis in ApoE knock-out mice. *J. Clin. Invest.* **99**:2752–2761.
37. Whitman, S.C., Ravisankar, P., Elam, H., and Daugherty, A. 2000. Exogenous interferon-gamma enhances atherosclerosis in apolipoprotein $E^{-/-}$ mice. *Am. J. Pathol.* **157**:1819–1824.
38. Upadhya, S., Mooteri, S., Peckham, N., and Pai, R.G. 2004. Atherogenic effect of interleukin-2 and antiatherogenic effect of interleukin-2 antibody in apo-E-deficient mice. *Angiology.* **55**:289–294.
39. Robertson, A.K., et al. 2003. Disruption of TGF-β signaling in T cells accelerates atherosclerosis. *J. Clin. Invest.* **112**:1342–1350.
40. Inagaki, Y., et al. 2002. Interferon-gamma-induced apoptosis and activation of THP-1 macrophages. *Life Sci.* **71**:2499–2508.
41. Wulff, H., et al. 2003. The voltage-gated Kv1.3 K^+ channel in effector memory T cells as new target for MS. *J. Clin. Invest.* **111**:1703–1713.
42. Nicolaou, S.A., Neumeier, L., Peng, Y., Devor, D., and Conforti, L. 2007. The Ca^{2+}-activated K^+ channel KCa3.1 compartmentalizes in the immunological synapse of human T lymphocytes. *Am. J. Physiol. Cell Physiol.* **292**:C1431–C1439.
43. Cruse, G., Duffy, S.M., Brightling, C.E., and Bradding, P. 2006. Functional KCa3.1 K^+ channels are required for human lung mast cell migration. *Thorax.* **61**:880–885.
44. Schwab, A., et al. 2006. Subcellular distribution of calcium-sensitive potassium channels (IK1) in migrating cells. *J. Cell. Physiol.* **206**:86–94.
45. Si, H., et al. 2006. Impaired endothelium-derived hyperpolarizing factor-mediated dilations and increased blood pressure in mice deficient of the intermediate-conductance Ca^{2+}-activated K^+ channel. *Circ. Res.* **99**:537–544.
46. Wojtulewski, J.A., et al. 1980. Clotrimazole in rheumatoid arthritis. *Ann. Rheum. Dis.* **39**:469–472.
47. Makita, K., et al. 1994. Experimental and/or genetically controlled alterations of the renal microsomal cytochrome P450 epoxygenase induce hypertension in rats fed a high salt diet. *J. Clin. Invest.* **94**:2414–2420.
48. Imai, T., et al. 2001. Vascular smooth muscle cell-directed overexpression of heme oxygenase-1 elevates blood pressure through attenuation of nitric oxide-induced vasodilation in mice. *Circ. Res.* **89**:55–62.
49. Begenisich, T., et al. 2004. Physiological roles of the intermediate conductance, Ca^{2+}-activated potassium channel Kcnn4. *J. Biol. Chem.* **279**:47681–47687.
50. Cook, S.J., and Lockyer, P.J. 2006. Recent advances in Ca^{2+}-dependent Ras regulation and cell proliferation. *Cell Calcium.* **39**:101–112.
51. Feske, S. 2007. Calcium signalling in lymphocyte activation and disease. *Nat. Rev. Immunol.* **7**:690–702.
52. Kauser, K., da Cunha, V., Fitch, R., Mallari,C., and Rubanyi, G.M. 2000. Role of endogenous nitric oxide in progression of atherosclerosis in apolipoprotein E-deficient mice. *Am. J. Physiol. Heart Circ. Physiol.* **278**:H1679–H1685.
53. Miura, H., et al. 2003. Diabetes mellitus impairs vasodilation to hypoxia in human coronary arterioles: reduced activity of ATP-sensitive potassium channels. *Circ. Res.* **92**:151–158.
54. Miller, F.J., Jr., Dellsperger, K.C., and Gutterman, D.D. 1998. Pharmacologic activation of the human coronary microcirculation in vitro: endothelium-dependent dilation and differential responses to acetylcholine. *Cardiovasc. Res.* **38**:744–750.
55. Larsen, B.T., et al. 2008. Hydrogen peroxide inhibits cytochrome P450 epoxygenases interaction between two endothelium-derived hyperpolarizing factors. *Circ. Res.* **102**:59–67.
56. Ray, J.L., Leach, R., Herbert, J.M., and Benson, M. 2002. Isolation of vascular smooth muscle cells from a single murine aorta. *Methods Cell Sci.* **23**:185–188.
57. Novak, N., et al. 2003. Evidence for a differential expression of the FcepsilonRIgamma chain in dendritic cells of atopic and nonatopic donors. *J. Clin. Invest.* **111**:1047–1056.
58. Mathy, N.L., Bannert, N., Norley, S.G., and Kurth, R. 2000. Cutting edge: CD4 is not required for the functional activity of IL-16. *J. Immunol.* **164**:4429–4432.
59. Steffens, S., et al. 2005. Low dose oral cannabinoid therapy reduces progression of atherosclerosis in mice. *Nature.* **434**:782–786.
60. Elbashir, S.M., et al. 2001. Duplexes of 21-nucleotide RNAs mediate RNA interference in cultured mammalian cells. *Nature.* **411**:494–498.